# Accelerating chemical waves accompanied by traveling hydrodynamic motion and surface deformation

Hidetoshi Miike and Hideaki Yamamoto

*Department of Electrical and Electronic Engineering, Yamaguchi University, Ube 755, Japan*

Shoichi Kai

*Department of Electrical Engineering, Kyushu Institute of Technology, Kitakyushu 804, Japan*

Stefan C. Müller

*Max-Planck-Institut für Molekulare Physiologie, Rheinlanddamm 201, D-4600 Dortmund 1, Germany*

A chemical trigger wave is initiated which propagates with accelerating speed in a thin liquid layer of the oscillatory Belousov-Zhabotinsky reaction. The localized phase gradient of the oscillation and induction of a hydrodynamic motion traveling with the chemical wave are possible causes for the acceleration. Evidence for pronounced hydrodynamic flow is supplied by digital processing of images visualizing flow patterns under the microscope. Surface deformations due to the hydrodynamic motion are analyzed by Mach-Zehnder interferometry.

## I. INTRODUCTION

Spatiotemporal organization in nonequilibrium systems is of great current interest in many disciplines of science [1]. A well-known example of structures forming far from thermodynamic equilibrium is found in the chemical waves traveling in the Belousov-Zhabotinsky (BZ) reaction [2]. In an unstirred and shallow layer of this solution, circular and spiral-shaped chemical waves are observed. Their occurrence has been treated theoretically by modeling the coupling of reaction and diffusion [3,4].

Pattern dynamics due to the interaction of reaction-diffusion waves with convective flow has attracted increasing attention. Convective effects accompanied by chemical-wave propagation in covered and uncovered shallow layers have been studied by several authors [2,5–7]. Novel hydrodynamic phenomena in chemical waves were detected in systems minimizing evaporative cooling by a protective cover: an oscillatory flow induced by periodic passage of spiral wave trains [8,9] and hydrodynamic flow traveling with a circular wave [10]. However, in spite of several experimental and theoretical approaches [11–13], the mechanism of this type of hydrodynamic phenomenon has not yet been clarified.

Here we report on the initiation of a chemical trigger wave with pronounced amplitude, the speed of which is accelerated during propagation. This acceleration is associated with a hydrodynamic motion in the liquid layer, as detected by computerized velocimetry based on image sequence processing of the propagating chemical waves in the investigated excitable BZ-solution layer. Furthermore, we apply Mach-Zehnder interferometry to measure propagating surface deformations induced by the spontaneously driven convection. Surface deformations, wave velocity, and induced hydrodynamic motion are found to depend strongly on the time when waves are triggered after mixing the solution.

## II. EXPERIMENTS

The preparation of a "classical" excitable BZ solution with an initial mixture of 48 m$M$ NaBr, 340 m$M$ NaBrO$_3$, 95 m$M$ CH$_2$(COOH)$_2$, and 378 m$M$ H$_2$SO$_4$ has been previously described [7,8]. For measuring hydrodynamic flow, polystyrene particles (diameter 0.5 $\mu$m) serving as scattering centers were mixed into the solution. Subsequently, the catalyst and indicator ferroin (3.5 m$M$) was added for starting the reaction ($t = 0$). Immediately afterward, a volume of the mixture producing a layer of about 0.85 mm depth was poured into a Petri dish (diameter 7 cm). In the layer thus prepared, one circular wave was triggered by immersing a silver wire (diameter 0.2 mm) for a given time period (1–10 s). Fresh mixtures were prepared for every new experiment using super pure water (relative resistance 20 M$\Omega$ m) obtained from Advantec Aquarius GSU-901 which filters out dust particles by a 0.5-$\mu$m Millipore filter. The room temperature was kept at 25±1 °C. We note here that the used mixture is not strictly excitable, in that long-period bulk oscillations (5–8 min) occur if no wave is triggered at all in the layer.

For quantitative measurements of the chemical dynamics, two-dimensional (2D) spectrophotometry [7], 2D velocimetry based on image sequence processing [8,12], and Mach-Zehnder interferometry are introduced. The propagating characteristics of the chemical waves are observed by a CCD camera with a 490-nm bandpass filter according to a standard procedure. For measuring hydrodynamic flow, computerized velocimetry based on image sequence processing is applied. The apparatus consists of a He-Ne laser, an inverse microscope, a CCD camera, a personal computer with image acquisition board, and a work station network. The details of the system configuration and the velocimetry are reported elsewhere [8,12]. In order to obtain quantitative evidence and global properties of the surface deformation due to the hydrodynamic flow induced by chemical reaction, a

Mach-Zehnder interferometer (MZI) is used which uti-
lizes the surface of the reactive layer as the lower mirror.
The upper mirror and two half mirrors in this setup have
the maximum grade of $\lambda/20$ ($\lambda = 6328$ Å) for both flat-
ness and uniformity over an area of 70 mm in diameter.
By the phase difference of the light reflected at a flat sur-
face, a periodic interference pattern with equidistant
stripes (fringes) is observed on the the screen. Any sur-
face deformation results in a corresponding fringe shift.
From the shifting direction one can determine whether
the surface deformation is a hill (convex) or a valley (con-
cave). During chemical wave propagation, the dynamic
behavior of the interference fringe pattern is monitored
by a CCD camera and recorded on a video tape recorder
(JVC Co., BR8600).

### III. RESULTS AND DISCUSSION

Experiments were carried out by triggering one circu-
lar wave close to the boundary of the Petri dish with a
silver wire. By carefully cleaning the dish, spontaneous
initiation of other waves was suppressed. When the cir-
cular wave is excited by a normal triggering procedure
(e.g., by immersing the silver for 1 s in the BZ solution), a
constant propagation velocity of chemical activity is ob-
served. However, immersing the wire for a longer dura-
tion (e.g., for 10 s) a very rapid and accelerating chemical
wave appears in the solution layer, as shown in the pic-
ture sequence of Fig. 1. The pronounced reactive front is
here referred to as "big wave." Remarkable characteris-
tics of this wave are (1) a broad and big oxidized front re-
gion [about 1 cm, see Fig. 1(c), (2) rapid wave propaga-
tion with accelerating speed (see Fig. 2), and (3) spon-
taneous formation of spiral structures behind the passing
wave [see Fig. 1(d)]. For the triggering conditions of the
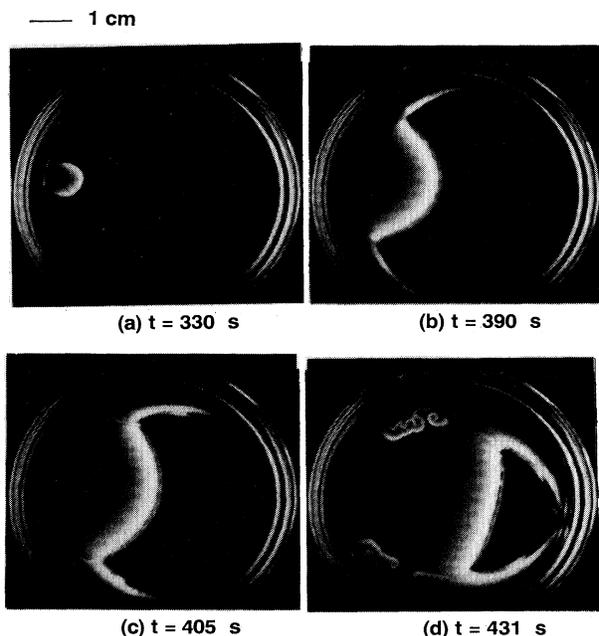big wave it is important that a clean dish and pure water

are used, the immersing period of the wire is longer than
5 s, the delay between solution preparation and trigger
time is more than 3 min, and only one pulse keeps travel-
ing through the layer.

The propagation velocities of the wave front were mea-
sured as a function of time after mixing the catalyst, and
its temporal change is summarized in Fig. 2. It shows an
accelerating propagation of the big wave [Figs. 2(b)–2(d)]
and a strong dependence on the trigger time $t_{tr}$ at which
a circular wave is excited at one end of the dish. As $t_{tr}$ is
delayed, the rate of change of the wave propagation ve-
locity increases. For comparison, the propagation veloci-
ty of the ordinary trigger wave is also shown [Fig. 2(a)],
which remains almost constant and does not depend on
$t_{tr}$.

Following previous studies on the possible role of hy-
drodynamic phenomena [10,12], we carried out measure-
ments of the motion of suspended scattering particles
near the surface of the solution layer at the center of the
dish. We found that, in fact, a pronounced flow is in-
duced by the propagating wave, as shown in the temporal
traces of Fig. 3. Curve (a) represents the case of ordinary
trigger wave (trigger time less than 1 s), which is accom-
panied by only moderate hydrodynamic flow (below 100
$\mu m/s$ [10]). On the other hand, very rapid hydrodynamic
motion is associated with the big wave propagation [Figs.
3(b) and 3(c)]. The maximum flow velocity can attain al-
most 3000 $\mu m/s$. Thus, it is almost 30 times faster than
that induced by an ordinary wave. Due to this rapid flow
there appear, in the wake of the big wave, spatial inho-
mogeneities which finally result in front breaking and
subsequent formation of spirals.

Investigation of wave propagation with a Mach-
Zehnder interferometer reveals that ordinary trigger
wave passage through the observation area (diameter 25
mm) results in an interference pattern of parallel fringes
without any modulation, i.e., surface deformations are
not detectable. By contrast, for the big wave, a distinc-
tive change of the width and periodicity in the fringe pat-
tern occurs, as shown in the image sequence of Fig. 4.
The expansion and contraction of the fringe spacing in
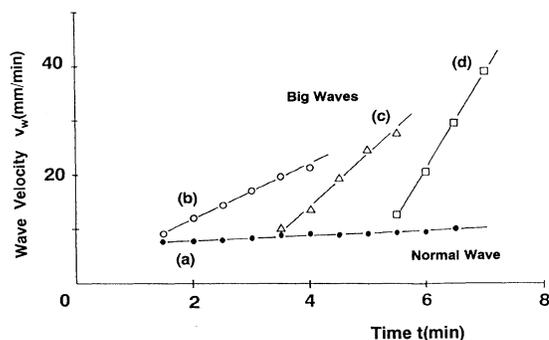the course of time corresponds to the convex and concave

—— 1 cm



(a) t = 330 s          (b) t = 390 s

(c) t = 405 s          (d) t = 431 s

FIG. 1. Picture sequence showing front propagation of a "big
wave," triggered by 10 s immersion of silver wire at trigger time
$t_{tr} = 5$ min (after mixing the catalyst to the BZ regent).



FIG. 2. Temporal change of propagation velocity ($v_w$) of a
wave. (a) Ordinary wave triggered at $t_{tr} = 1$ min after mixing
(by 1 s immersion); (b), (c), and (d) big waves triggered at $t_{tr} = 1$,
3, and 5 min (by about 10 s immersion), respectively. The veloc-
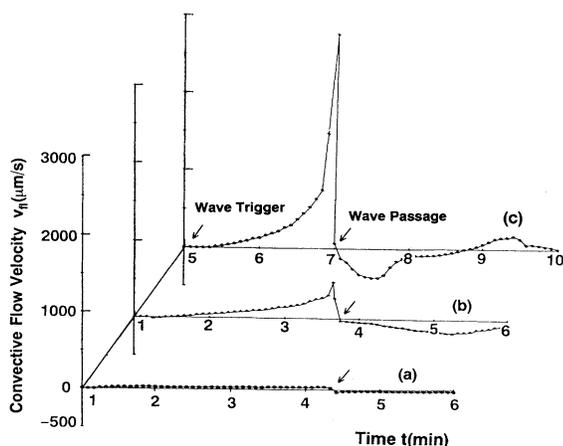ity of the big waves is accelerated with time and strongly de-
pends on the trigger time.

FIG. 3. Temporal traces of hydrodynamic motion velocity $(v_{fl})$ induced by chemical-wave propagation. (a) Ordinary wave triggered at $t_{tr} = 1$ min after mixing; (b) and (c) big waves triggered at $t_{tr} = 1$ and 5 min (10 s immersion), respectively. The velocity $v_{fl}$ associated with the big wave is almost 30 times faster than that of the ordinary wave.

shapes of surface deformations, respectively. In this example, the circular wave is triggered 157 s after mixing the catalyst, and the surface deformation $H$ propagates across the observation area with a velocity of approximately 300 $\mu$m/s. The temporal trace of $H$ shown in Fig. 5 was obtained at the observation point marked with a cross in Fig. 4(a). The maximum deformation $H_{max}$ is 2.8 $\mu$m, which is about 0.3% of the solution depth. It travels across the detection area with a visible width of 1.2 cm. The ratio between height and width is approximately $5 \times 10^3$, which emphasizes the smallness of the deformation. According to the simultaneous observation with a
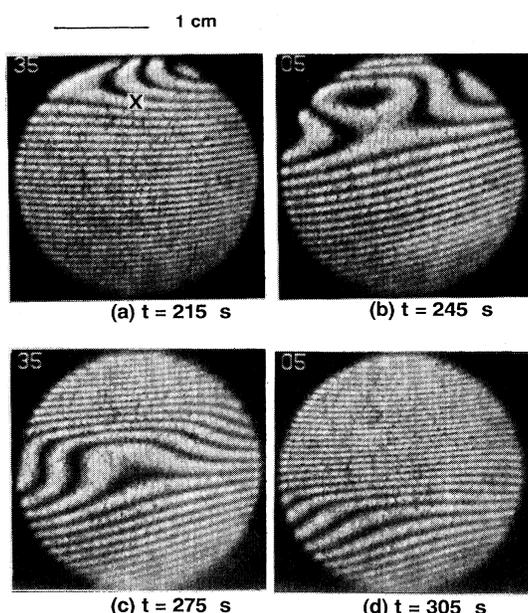


FIG. 4. Distortion of fringe pattern in a Mach-Zehnder interferometer caused by the big wave propagation from the top to the bottom; $t_{tr} = 157$ s.
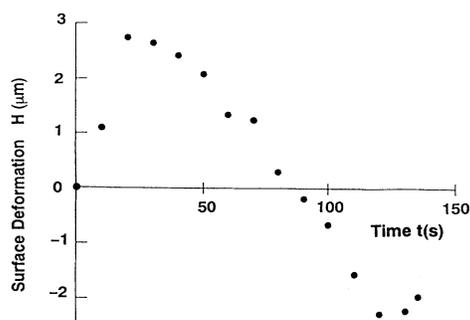


FIG. 5. Temporal trace of the surface deformation $H$ caused by the big wave propagation; origin of time axis chosen at trigger time $t_{tr} = 157$ s. Maximum deformation $H_{max} = 2.7$ $\mu$m.

real image, $H_{max}$ appears at a distance of $\Delta x = 1$ mm in front of the corresponding wave front, comparable to the layer depth. This supports the existence of a convection role in the convex position.

The maximum deformation $H_{max}$ and the maximum propagation velocity $v_{max}$ of the big wave were measured for various trigger times $t_{tr}$. Figure 6 shows that the inverse values $1/H_{max}$ and $1/v_{max}$ depend linearly on $t_{tr}$. This leads to the empirical relationships ($H_{max}$ in $\mu$m,
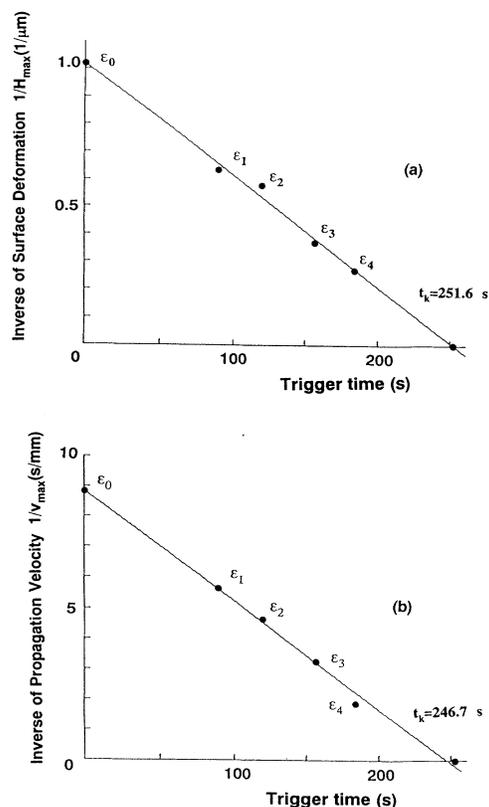


FIG. 6. Inverse of maximum deformation $H_{max}^{-1}$ (a), and of maximum propagation velocity $v_{max}^{-1}$ (b) of the big wave as a function of trigger time $t_{tr}$. Here, $\varepsilon_1$, $\varepsilon_2$, $\varepsilon_3$, and $\varepsilon_4$ show the measured points. the straight line is determined by linear regression. The values $\varepsilon_0$ and $t_k$ are obtained by extrapolation.

$v_{max}$ in mm/s, $t_{tr}$ in s)

$$1/H_{max} = -0.004\,05 t_{tr} + 1.02 \; , \tag{1}$$

$$1/v_{max} = -0.0358 t_{tr} + 8.83 \; . \tag{2}$$

By extrapolating Eq. (1) the divergent point of the deformation is estimated as $t_k = 251.6$ s. Almost the same value ($t_k = 246.7$ s) results from extrapolating Eq. (2). This points to a possibly simple analytical connection between $H_{max}$ and $v_{max}$, indicating a critical behavior which should be accounted for in the mechanistic understanding of the big wave. Especially, one has to consider that the BZ solution used here is not strictly excitable, but oscillates with a long period ($\sim 8$ min). Precise measurements around the critical time $t_k$ would be desirable. They are difficult, however, because the condition of isolated wave propagation in the hole solution layer cannot be easily maintained due to spontaneous initiation of waves in this critical situation. Once multiple waves are excited, the occurrence of the big wave and surface deformations are extremely reduced.

## IV. CONCLUDING REMARKS

The usual properties of the big wave cannot be explained on the basis of diffusion-reaction models alone. Most likely, the oscillatory nature of the BZ solution and the hydrodynamic flow [8–10] accompanied by the wave have to be taken into account. The formation of a "phase wave (pseudowave)" [14] and a "phase diffusion wave" [15], as observed in the latest phase of the reduced state of the oscillatory BZ solution, could explain the accelerating nature of the big wave. In fact, a very rapid propagation of a chemical wave was recently found in an oscillatory BZ-solution layer in which a phase gradient was artificially established by propagation of one circular wave [12] (after the wave propagation spatially nonsynchronous oscillation is realized in the solution which produces a global phase gradient). A second wave following the first one propagates with accelerating speed just as the big wave discussed here. However, this big wave can be distinguished clearly from the phase waves (including phase diffusion waves). In contrast to the phase waves, the big wave can be triggered at the early stage of the reduced state, and it is initiated in a homogeneously reduced BZ-solution layer in the absence of any global phase gradient. The long duration of immersing a silver wire for its initiation ($\sim 10$ s) could establish a localized concentration gradient of $Br^-$ ions, and thus a phase gradient sufficient for local speed acceleration and simultaneous coupling to a hydrodynamic motion. Further acceleration of propagation speed by this motion is likely to occur. At the present stage no mechanistic explanation of this phenomenon is available, which calls for more detailed experimentation and modeling efforts on the chemically driven hydrodynamic motion and its coupling to reaction-diffusion patterns.

## ACKNOWLEDGMENT

[1] *Thermodynamic Theory of Structure, Stability and Fluctuations*, edited by P. Glansdorf and I. Prigogine (Wiley, New York, 1971).

[2] A. M. Zhabotinsky and A. N. Zaikin, J. Theor. Biol. **40**, 45 (1973).

[3] *Oscillations and Traveling Waves in Chemical Systems*, edited by R. J. Field and M. Burger (Wiley, New York, 1985).

[4] J. P. Keener and J. J. Tyson, Physica **21D**, 307 (1986).

[5] M. Orban, J. Am. Chem. Soc. **102**, 4311 (1980).

[6] K. I. Agladze, V. I. Krinsky, and A. M. Pertsov, Nature **308**, 834 (1984).

[7] S. C. Müller, Th. Plesser, and B. Hess, Ber. Bunsenges. Phys. Chem. **89**, 654 (1985).

[8] H. Miike, S. C. Müller, and B. Hess, Chem. Phys. Lett. **144**, 515 (1988).

[9] H. Miike, S. C. Müller, and B. Hess, Phys. Lett. **61**, 2109 (1988).

[10] H. Miike, S. C. Müller, and B. Hess, Phys. Lett. A **141**, 25 (1989).

[11] J. A. Pojman and I. R. Epstein, J. Phys. Chem. **94**, 4966 (1990).

[12] H. Miike, H. Yamamoto, M. Momota, and H. Hashimoto, in *Pattern Formation in Complex Dissipative Systems*, edited by S. Kai (World Scientific, Singapore, 1992), pp. 191–200.

[13] Th. Plesser, H. Wilke, and K. H. Winters, Chem. Phys. Lett. **200**, 158 (1992).

[14] M. L. Smoes, in *Dynamics of Synergetic Systems*, edited by H. Haken (Springer-Verlag, Berlin, 1980), pp. 80–96.

[15] J. M. Bodet, J. Ross, and C. Vidal, J. Chem. Phys. **86**, 4418 (1987).
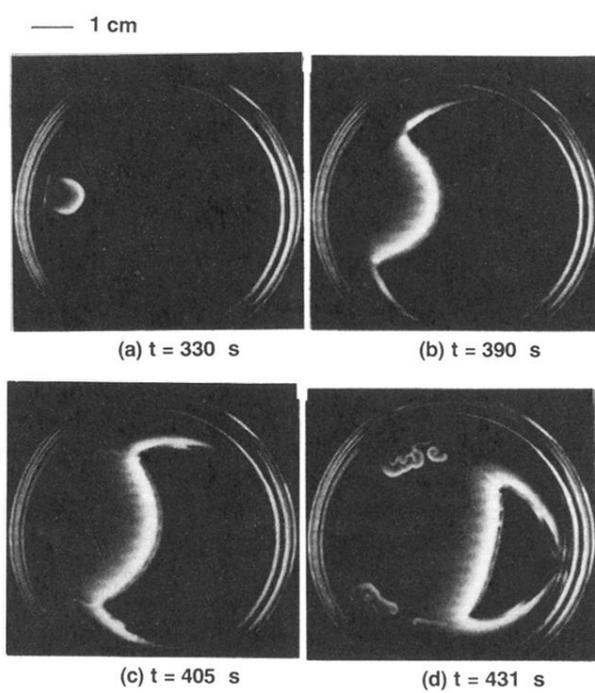
FIG. 1. Picture sequence showing front propagation of a "big wave," triggered by 10 s immersion of silver wire at trigger time $t_{tr} = 5$ min (after mixing the catalyst to the BZ regent).
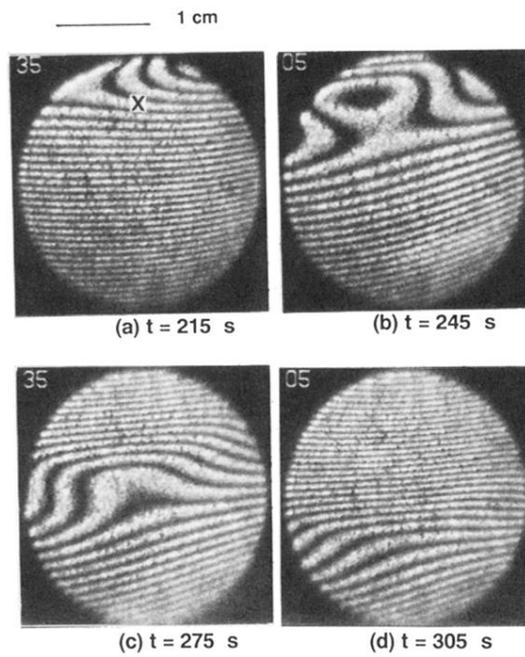
FIG. 4. Distortion of fringe pattern in a Mach-Zehnder interferometer caused by the big wave propagation from the top to the bottom; $t_{tr} = 157$ s.